Available online at www.sciencedirect.com

ScienceDirect

Ceramics International 40 (2014) 2551–2555

CERAMICS INTERNATIONAL

www.elsevier.com/locate/ceramint

Short communication

# Piezoelectric behavior of $(1-x)(PbMgNbO_3–PbZrTiO_3)–x(BaTiO_3)$ ceramics for energy harvester applications

Moon-Soon Chae[1], Jung-Hyuk Koh[1,2,*]

[1]Department of Electronic Materials Engineering, Kwangwoon University, Republic of Korea
[2]School of Electrical and Electronic Engineering, Chung-Ang University, Republic of Korea

Received 2 May 2013; received in revised form 26 June 2013; accepted 12 July 2013
Available online 21 July 2013

**Abstract**

The $Pb(Mg_{1/3}Nb_{2/3})O_3–Pb(Ti,Zr)O_3$ system near morphotropic phase boundary (MPB) can be expected to provide a high piezoelectric charge coefficient and electromechanical coupling coefficient. Therefore, it has been used as an excellent candidate for piezoelectric applications, including energy harvester applications. In this study, electric field-induced phase transition in $(1-x)(PbMgNbO_3–PbZrTiO_3)–x(BaTiO_3)$ ceramics in a relatively low field of 40 kV/cm will be discussed. XRD analysis showed tetragonal and rhombohedral perovskite structure of $PbMgNbO_3–PbZrTiO_3$ with $BaTiO_3$, indicated that phase transition was occurred with increasing $BaTiO_3$, component. Measurement of room temperature dielectric constant indicated a gradual increase with increasing $BaTiO_3$ content. The results show that the addition of $BaTiO_3$ is very effective in improving the dielectric and electric properties of $Pb(Mg_{1/3}Nb_{2/3})O_3–Pb(Ti,Zr)O_3$ system.


*Keywords:* C. Piezoelectric properties; D. $BaTiO_3$; PMN–PZT

## 1. Introduction

Lead magnesium niobate–lead zirconate titanate (Pb,Mg)$NbO_3$–(Pb,Zr)$TiO_3$ (PMN–PZT) ceramics are promising candidates for transducer applications due to their excellent piezoelectric and dielectric properties [1,2]. Generally, the conventional sintering process has limits regarding density compared with hot isostatic pressing and cold isostatic pressing. Among the perovskite ferroelectric materials, lead zirconate titanate (PZT) and barium titanate ($BaTiO_3$) ceramics have been investigated extensively due to their excellent properties. These two outstanding piezoelectric ceramic materials are suitable for different applications.

$BaTiO_3$ ceramics have been studied with various isovalent dopants. $BaTiO_3$ ceramics with both A and B sites substituted with different dopants in the perovskite structure have shown different phase transition temperatures [3]. $BaTiO_3$ has a stable tetragonal ferroelectric phase with a *c/a* value, the ratio of lattice parameters, of about 1.01, when the temperature is above 120 °C.

Perovskite-structured PZT has a Curie transition temperature near 350 °C, and is formed through binary solid solutions of ferroelectric $PbTiO_3$ ($T_c$≈490 °C) and antiferroelectric $PbZrO_3$ ($T_c$≈230 °C) phases. A morphotropic phase boundary in PZT divides the regions of the ferroelectric phase into two parts: a ferroelectric tetragonal phase region (Ti-rich side) and a rhombohedral phase region (Zr-rich side). Generally, $BaTiO_3$ ceramic has better mechanical properties than PZT, and the sintering temperature is also higher [4]. However, the piezoelectric charge coefficient of $BaTiO_3$ is lower than that of PZT.

The $Pb(Mg_{1/3}Nb_{2/3})O_3–Pb(Ti,Zr)O_3$ system near the morphotropic phase boundary can be expected to provide a high piezoelectric charge coefficient and electromechanical coupling coefficient. Therefore, it is an excellent candidate for power applications [5]. Recently, Ryu et al. reported on the effect of Yb doping on the high-power piezoelectric properties of PMN–PZT ceramics [6].

For the energy harvester applications, it is important to have high dielectric permittivity to obtain large energy capacities with piezoelectric materials. Since the energy generated can be increased by improving the capacitance of the piezoelectric materials, modulation of materials properties to improve the

*Corresponding author. Tel.: +82 2 940 5162; fax: +82 2 915 0566.
*E-mail addresses:* jhkoh@kw.ac.kr (J.-H. Koh).

0272-8842/$ - see front matter © 2013 Elsevier Ltd and Techna Group S.r.l. All rights reserved.
http://dx.doi.org/10.1016/j.ceramint.2013.07.062

dielectric permittivity can be a critical issue for energy harvester applications.

So far, there have been a limited number of reports on doped $PbMgNbO_3$–$PbZrTiO_3$ systems [7,8]. There have been no systematic studies on the phase development and dielectric properties of various compositions of $(1-x)(PbMgNbO_3$–$PbZrTiO_3)$–$x(BaTiO_3)$ (PMN–PZT–BT hereafter), which would help in identifying excellent electrical properties within this system. In the present study, PMN–PZT–BT was chosen to prepare solid solutions through a modified mixed-oxide method. The phase development and strain changes of the samples are investigated.

## 2. Experimental procedure

The stoichiometric $(1-x)(PbMgNbO_3$–$PbZrTiO_3)$–$x(BaTiO_3)$ ceramic compositions were prepared from (Pb,Mg)$NbO_3$, (Pb, Zr)$TiO_3$, and $BaTiO_3$ starting powders by mixed-oxide method ($x$=0, 0.1, 0.2, 0.3, 0.4 and 0.5). The $Pb_3O_4$, $ZrO_2$, $TiO_2$, $MgNb_2O_6$, and $BaCO_3$ powders with 99.9% purity were prepared as starting powders. To obtain the $PbMgNbO_3$–$PbZrTiO_3$ powder, the PbO, $ZrO_2$, $MgNb_2O_6$, and $TiO_2$ powders were ball-milled in a stiochiometric ratio, and then calcined at 850 °C for 2 h. For $BaTiO_3$ powder, $BaCO_3$ and $TiO_2$ were homogeneously mixed via ball-milling process with zirconia media in ethanol for 24 h. The mixture was dried and then calcined at 1300 °C for 2 h to form $BaTiO_3$. The PMN–PZT and BT powders for a given composition were weighed and then ball-milled using zirconia balls in ethanol as media for 24 h. The powders were calcined at 900 °C for 2 h. After that, the reacted material was additionally ball-milled to ensure a fine particle size before sintering. The dried powder was axially pressed into disks 12 mm in diameter and about 1.5 mm in thickness, with 5 wt% polyvinyl alcohol (PVA) as a binder. The pellets were stacked in a covered alumina crucible filled with PZT powders to prevent lead loss. Finally, the sintering was carried out at a sintering temperature for 2 h with 5 °C/min heating and cooling rates. The firing profile includes a 1-h dwelling time at 600 °C to burn out the binder. For optimization, the sintering temperature was varied between 1100 and 1200 °C depending upon the compositions. The bulk density of the sintered specimen was measured using Archimedes' principle. The phase formations of the sintered samples were analyzed by X-ray diffraction analysis with a Cu Kα radiation source (Rigaku Model D/MAX-2500V/PC, Japan).

For electrical measurements, silver paste was coated onto both sides of the sintered samples. The dielectric permittivity and loss of the unpoled ceramics were measured using an impedance analyzer (HP4294A, Hewlett-Packard Company) at different frequencies ranging from 1 kHz to 1 MHz at room temperature. The temperature dependence of the dielectric constant was obtained using a programmable automatic LCR meter (FLUKE PM 6304). $P$(E) and $S$(E) curves, where $P$ and $S$ denote the polarization and strain, respectively, were obtained at 50 mHz in silicon oil with the aid of a Sawyer–Tower circuit to apply an electric field with a triangular waveform. The piezoelectric charge coefficient $d_{33}$ was measured using a pieozo-$d_{33}$ meter (YE 2730A, USA) after poling at 120 °C for 30 min at an applied electric field of 4 kV/mm. The planar electromechanical coupling factor $k_p$ was calculated according to IEEE standards using an impedance analyzer (HP 4294A).

## 3. Result and discussion

The crystalline properties of $(1-x)$(PMN–PZT)–$x$BT ceramics were analyzed by XRD, as shown in Fig. 1(a). The peak positions and intensities of XRD patterns were changed according to the amount and chemical composition of the phases present. From the XRD patterns, the PMN–PZT ceramic was identified as a single-phase material with a perovskite structure having tetragonal symmetry. With increasing BT content up to 20%, the diffraction peaks shifted towards a lower angle, and the diffraction peak around a $2\theta$ value of 43–46° was split (as shown in Fig. 1(b)). A diffused phase transition was observed with increasing BT component. This observation suggests that the 0.8(PMN–PZT)–0.2BT composition may lead to move morphotropic phase boundary (MPB) between the antiferroelectric (AFE) tetragonal and ferroelectric (FE) rhombohedral PMN–PZT phases. Fig. 1(b) shows the evolution of the (200) and (002) peaks as a function of the $(1-x)$(PMN–PZT)–$x$BT composition over the $2\theta$ range of 43–46°. The graph indicates the appearance of a weak pseudocubic peak due to the superposition of the tetragonal and cubic (200) peak. The XRD patterns with a low degree of BT content ($0.1 \le x \le 0.2$) showed the character of tetragonal AFE phase in all samples, as shown in Fig. 1(b). With increasing BT content, the intensity ratio of the (200) and (002) peak tends to decrease when $x=0.3$, and it seems that the ceramic has a tendency to transform into pseudocubic phase. This indicated that the $(1-x)$(PMN–PZT)–$x$BT ceramics have an increased lattice parameter $c$ and tetragonality when $x$ is 0.2. In addition, AFE and FE phase transition are located near $0.2 \le x \le 0.3$.

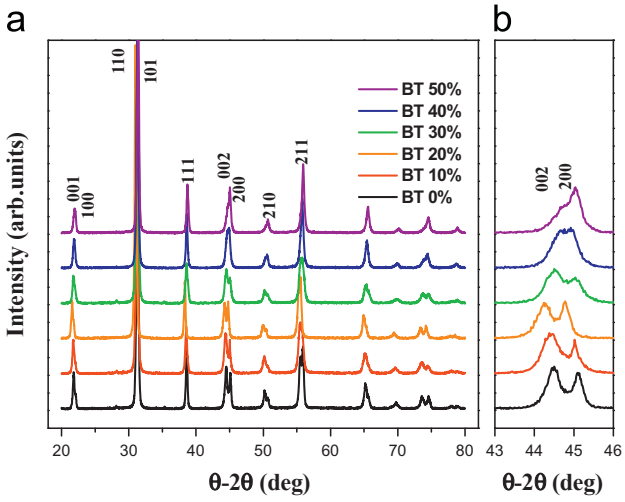


Fig. 1. (a) XRD patterns of $(1-x)$(PMN–PZT)–$x$BT ceramics as a function of BT content and (b) XRD patterns of $(1-x)$(PMN–PZT)–$x$BT ceramics (43–46°).

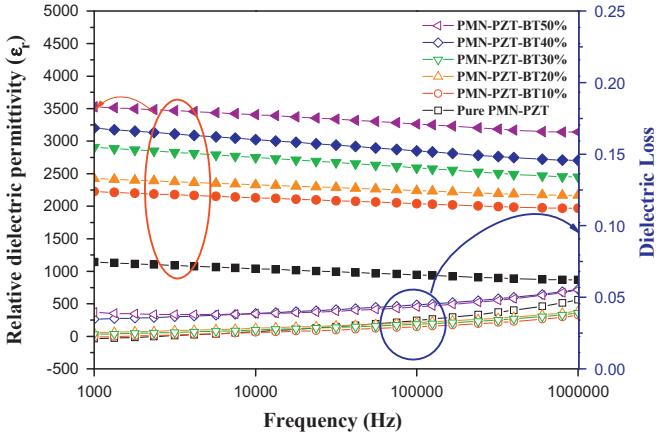


Fig. 2. Frequency-dependent dielectric permittivity and loss tangent of $(1-x)$(PMN–PZT)–$x$BT ceramics.

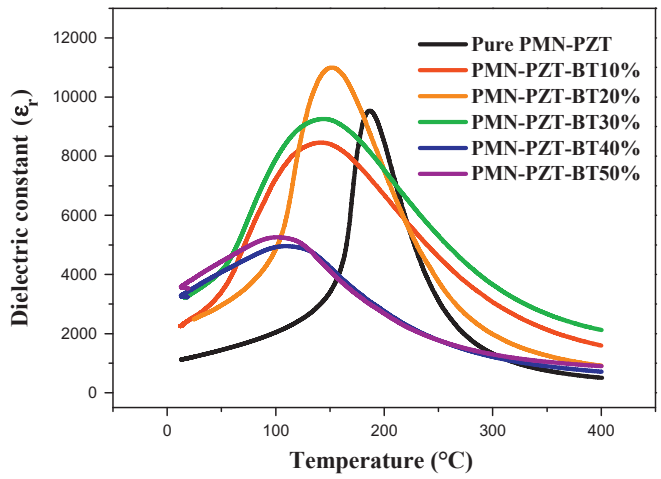


Fig. 3. Temperature-dependent dielectric permittivity of $(1-x)$(PMN–PZT)–$x$BT ceramics.

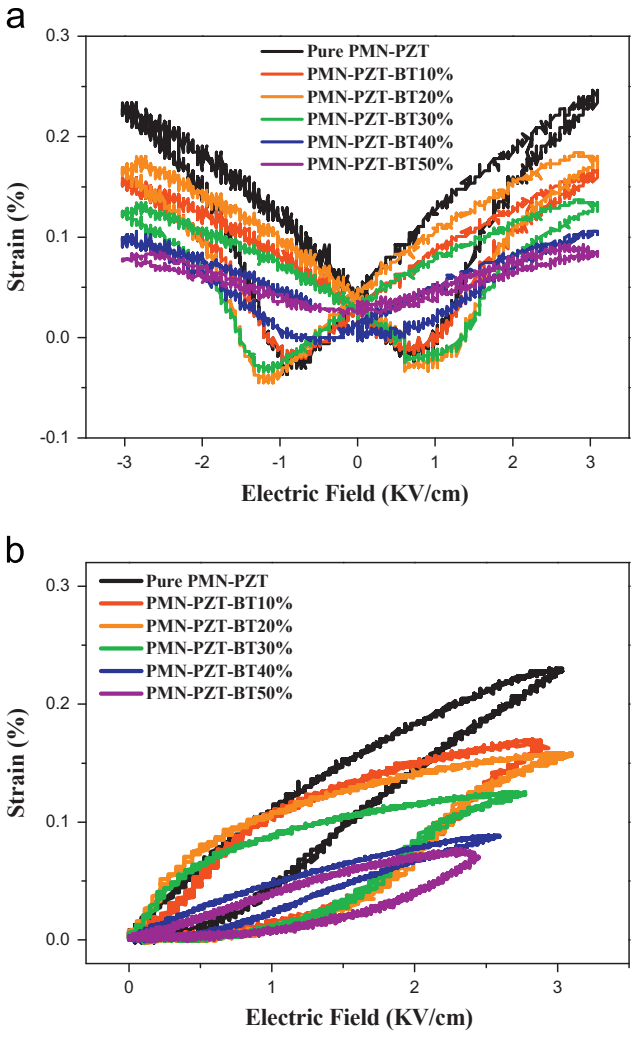


Fig. 4. (a) Bipolar and (b) unipolar strains versus electric field for $(1-x)$(PMN–PZT)–$x$BT ceramics by varying the BT content.

Fig. 2 shows the frequency-dependent dielectric permittivity ($\varepsilon_r$) and dielectric loss of the $(1-x)$(PMN–PZT)–$x$BT ceramic system. The dielectric property observed with increasing BT component at room temperature. The dielectric permittivity $\varepsilon_r$ of the $(1-x)$(PMN–PZT)–$x$BT ceramics at 1 MHz ranged from 867 (pure PMN–PZT) to 3140 (0.5(PMN–PZT)–0.5BT), whereas the value of the dielectric loss was in the range of 0.0374–0.0556. With increasing frequency range from 1 kHz to 1 MHz, the dielectric permittivity decreased. The decrease in the value of $\varepsilon_r$ can be explained based on the decrease in polarization with the increase in frequency. The polarization of a dielectric material is the sum of the contributions of dipolar, electronic, ionic, and interfacial polarization [9].

The temperature-dependent dielectric permittivity of the $(1-x)$(PMN–PZT)–$x$BT ceramics is displayed in Fig. 3. The Curie temperatures and maximum dielectric permittivity of the pure PMN–PZT ceramics in this work were 186 °C and 9535, respectively. With increasing BT content, the Curie temperature shifts gradually to lower temperatures, and the dielectric peak becomes broader, indicating an increasing diffused phase transition. As mentioned, a combination of PMN–PZT with BT induces dielectric peak broadening. For a normal ferroelectric such as PMN–PZT and BT, beyond the Curie temperature, the dielectric permittivity behaves according to the Curie–Weiss law

$$\varepsilon = c/(T-T_0) \tag{1}$$

where $c$ is the Curie constant and $T_0$ is the Curie–Weiss temperature [10]. For a ferroelectric with a diffuse phase transition, the following equation describes the dielectric permittivity:

$$1/\varepsilon = (T-T_m)^2 \tag{2}$$

This has been shown to be valid over a wide temperature range, in contrast to the normal Curie–Weiss law. In Eq. (2), $T_m$ is the temperature at which the dielectric constant is the maximum value.

The composition-dependent bipolar electric field-induced strain curves are provided in Fig. 4(a). The ceramic with $x=0$ shows a bipolar strain curve similar to that of a typical butterfly-shaped strain hysteresis loop. At lower BT content ($x\leq 0.3$); the samples have coexisting $R$–$T$ symmetry. And then, the negative strain significantly moved to zero. The negative strain increased

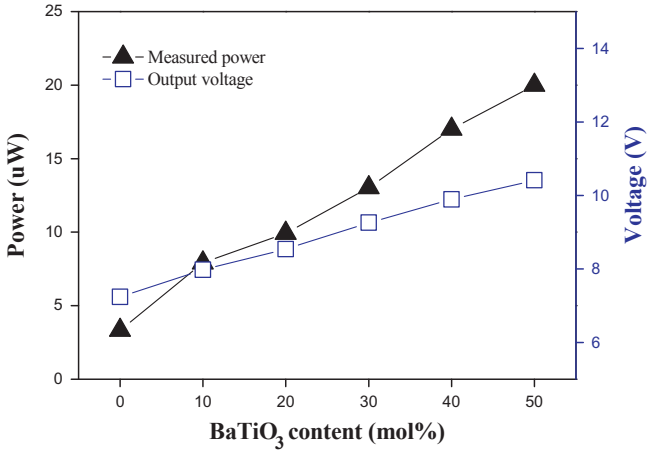


Fig. 5. The Generated output power of $(1-x)$(PMN–PZT)–$x$BT ceramics by varying the BT content.

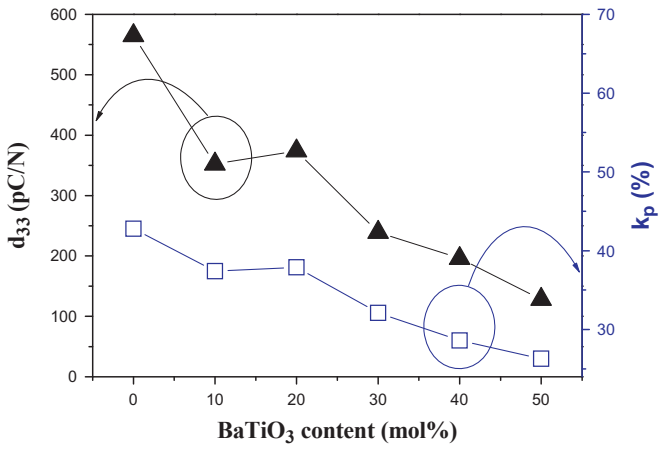


Fig. 6. Piezoelectric charge coefficients $d_{33}$ and piezoelectric planar coupling coefficients $k_p$ of $(1-x)$(PMN–PZT)–$x$BT ceramics by varying the BT content.

gradually with increase in BT content ≥0.3. Then, the structure changed to pseudocubic phase at $x=0.5$. The electric field-induced phase transition between antiferroelectric and ferroelectric contributed to the strain properties. So that the electric field-induced strain (EFIS) was also decreased with increasing the BT content. It is indicated that the negative strain is related to domain back-switching during bipolar cycles [11]. Fig. 4(b) illustrates the unipolar electric field-dependent strain curves for the poled $(1-x)$(PMN–PZT)–$x$BT ceramics, and summarizes the variations of the maximum strain at 3 kV/cm.

The piezoelectric strain ($S$) is calculated by the following equation:

$$S = s^E T + dE \tag{3}$$

where the $s^E T$ is the mechanical compliance of the component similarly to any mechanical component. The $dE$ is the piezoelectric effect. The composition-dependent strain ratio $S_{max}/E_{max}$ of the $(1-x)$(PMN–PZT)–$x$BT ceramics decreased with BT content (from 697 to 278 pm/V). This decreased electric field-dependent strain behavior probably comes from the decreased piezoelectric properties by increasing the BT content.

Fig. 5 exhibits the output power generated from the $(1-x)$(PMN–PZT)–$x$BT ceramics by increasing the BT content. The generated maximum output voltage from these devices was around 7.24–10.41 V. The energy power can be calculated from the generated output voltage. When solving for output power ($P$) by using the equation given by

$$P = 1/2 \times CV^2 \times f \tag{4}$$

where $C$ is the relative dielectric permittivity of $(1-x)$(PMN–PZT)–$x$BT, $V$ is the generated output voltage, and $f$ is the operating frequency (110 Hz). The dependence of output power on the BT composition is shown in Fig. 5. The generated output power of the $(1-x)$(PMN–PZT)–$x$BT ceramics are around 3.34–20.0 μW, depending on the BT content. As shown in the figure, the generated energy was increased as the BT mol% was increased. It seems that this increased energy comes from the increased relative dielectric permittivity. Since the relative dielectric permittivity of BT is much higher than that of PMN–PZT ceramics, the increased BT content enhanced the relative dielectric permittivities of the $(1-x)$(PMN–PZT)–$x$BT ceramics.

Fig. 6 shows the piezoelectric constant $d_{33}$ and planar electromechanical coefficient $k_p$ of $(1-x)$(PMN–PZT)–$x$BT ceramics as a function of BT content. The piezoelectric constant $d_{33}$ showed a maximum value of 565 pC/N when the amount of BT was 0%, and decreased with increasing BT content.

The electromechanical coupling factor ($k_p$) is calculated by the following equation [11]:

$$1/k_{p^2} = a \times f_r/(f_a - f_r) + b \tag{5}$$

where $f_r$ is the resonance frequency, $f_a$ is the anti-resonance frequency, $a=0.395$ and $b=0.574$ for planar ($k_p$) mode. The dependence of $k_p$ on the BT composition is shown in Fig. 6. The electromechanical coupling factor was decreased with increasing BT content (from 42.8% to 26.3%).

We have investigated the piezoelectric and structural properties of $(1-x)$(PMN–PZT)–$x$BT ceramics by increasing the BT content. We have found that the piezoelectric properties and generated output power have a strong dependence on the BT compositions.

## 4. Conclusions

Piezoelectric perovskite $(1-x)$(PMN–PZT)–$x$BT ceramics have been investigated. $(1-x)$(PMN–PZT)–$x$BT ceramics ($x=0$, 0.1, 0.2, 0.3, 0.4 and 0.5) were prepared by a conventional mixed-oxide method. The phase formation behavior, crystal structure, dielectric, electric field-induced strain properties and generated output power were investigated, which indicated that PMN–PZT–BT forms a series of continuous solid solutions. Also dielectric permittivity was increased with increasing BT contents at room temperature. The dielectric properties measured under stress-free conditions at room temperature show a gradual increase of the dielectric permittivity with increasing BT component, while the dielectric loss did not differ significantly. The bipolar and unipolar strain and the piezoelectric properties of the $(1-x)$(PMN–PZT)–$x$BT ceramics

decreased with increasing BT content, while the generated output power increased.

## Acknowledgment

This work was supported by a grant from the National Research Foundation of Korea (NRF), funded by the Korean government (MEST) (No. 2011-0029625).

## References

[1] R. Yimnirun, S. Ananta, P. Laoratanakul, Journal of the European Ceramic Society 25 (2005) 541.
[2] V. Koval, C. Alemany, J. Briancin, H. Brunckova, K. Saksl, Journal of the European Ceramic Society 23 (2003) 1157.
[3] B. Jaffe., W.R. Cook, H. Jaffe, Piezoelectric Ceramics, Academic Press, London, 1971.
[4] G.H. Haertling, Journal of the American Ceramic Society 82 (1999) 797.
[5] F. Tomoaki, S. Hiroshi, A. Masatoshi, Japanese Journal of Applied Physics 38 (1999) 3596.
[6] J. Ryu, H.W. Kim., K. Uchino, J. Lee, Japanese Journal of Applied Physics 42 (2003) 1307.
[7] E.M. Sabolsky, A.R. James, S. Kwon, S. Trolier-McKinstry, G. L. Messing, Applied Physics Letters 78 (2001) 2251.
[8] T. Richter, S. Denneler, C. Schuh, E. Suvaci, R. Moos, Journal of the American Ceramic Society 91 (2008) 929.
[9] A.K. Singh, T.C. Goel, R.G. Mendiratta, O.P. Thakur, C. Prakash, Journal of Applied Physics 91 (2002) 6626.
[10] G.H. Haertling, Journal of the American Ceramic Society 82 (1999) 797.
[11] Z. Yang, B. Liu, L. Wei, Y. Hou, Materials Research Bulletin 43 (2008) 81.